



HAL
open science

Processes controlling the shape of ash particles: Results of statistical IPA

S.C. Jordan, Tobias Dürig, Raymond AF Cas, Bernd Zimanowski

► **To cite this version:**

S.C. Jordan, Tobias Dürig, Raymond AF Cas, Bernd Zimanowski. Processes controlling the shape of ash particles: Results of statistical IPA. *Journal of Volcanology and Geothermal Research*, 2014, 288, pp.19-27. 10.1016/j.jvolgeores.2014.09.012 . hal-02107309

HAL Id: hal-02107309

<https://uca.hal.science/hal-02107309>

Submitted on 2 Dec 2022

HAL is a multi-disciplinary open access archive for the deposit and dissemination of scientific research documents, whether they are published or not. The documents may come from teaching and research institutions in France or abroad, or from public or private research centers.

L'archive ouverte pluridisciplinaire **HAL**, est destinée au dépôt et à la diffusion de documents scientifiques de niveau recherche, publiés ou non, émanant des établissements d'enseignement et de recherche français ou étrangers, des laboratoires publics ou privés.



Distributed under a Creative Commons Attribution - NonCommercial - NoDerivatives 4.0 International License

Processes controlling the shape of ash particles: Results of statistical IPA

S.C. Jordan ^{b,*}, T. Dürig ^c, R.A.F. Cas ^a, B. Zimanowski ^d

^a School of Geosciences, Monash University, 3800 Victoria, Australia

^b Laboratoire Magmas et Volcans (LMV), 63080 Clermont-Ferrand, France

^c Institute of Earth Sciences, University of Iceland, 101 Reykjavík, Iceland

^d Physikalisch Vulkanologisches Labor, Universität Würzburg, 97070 Würzburg, Germany

Ash particles have unique morphologies and shapes that are characteristic of certain fracture mechanisms and can be used to identify the type of fragmentation such as magmatic brittle or ductile fragmentation and phreatomagmatic molten fuel coolant interaction type fragmentation. Identifying these two different fragmentation processes is especially important in complex volcanic systems where both fragmentation processes can occur. In this study, image parameter analysis and statistical parameter analysis are used to compare ash particles from standardised magma fragmentation experiments with natural ash particles from the Pleistocene Lake Purrumbete maar, southeastern Australia. The pyroclastic Lake Purrumbete maar sequence contains various deposit types that show evidence for changing eruption conditions, therefore it is of a main interest to determine the main fragmentation mechanism that formed these deposits. A comparison with experimental ash particles revealed that Lake Purrumbete ash particles show significant differences from experimental samples of magmatic brittle type fragmentation, whereas they show no significant differences from phreatomagmatic molten fuel coolant interaction type fragmentation samples, indicating a predominance of phreatomagmatic fragmentation during the eruption of Lake Purrumbete. The experiments further show that pre-existing stresses also influence the particle shape and may be the reason for the absence of a significant similarity between most of the particle populations.

1. Introduction

Abundant fine ash is formed by brittle fragmentation during the most energetic eruption mechanism of both magmatic and phreatomagmatic origin (Zimanowski et al., 2003; Büttner et al., 2006). Büttner et al. (2006) showed that the thermodynamic theory of dynamic fragmentation by Yew and Taylor (1994) can be used to explain the process of magmatic fragmentation according to the principles of thermodynamics. According to Yew and Taylor (1994), the breakup of the material into particles is caused by internal strain of the material, where the size of the resulting particles is dependent on the strain rate; the higher the strain rate, the smaller the resulting particle size. Fragmentation during phreatomagmatic eruptions is caused by the interaction of magma and water in the way of molten fuel coolant interaction (MFCI), where the magma is cooled instantly at the magma/water interface and quenches, while the water evaporates. Fragmentation is caused by rapid expansion of super-heated water and simultaneous magma quenching (Wohletz, 1983; Zimanowski et al., 1997; Büttner et al., 1999). Graettinger et al. (2013) showed that both magmatic and phreatomagmatic fragmentation

mechanisms can be active during a single eruption and facilitate each other. Both processes may also lead to the exposure of fresh melt to water causing fragmentation of the melt by quench granulation (Graettinger et al., 2013). The complicated interplay of these different fragmentation processes will form deposits with different types of pyroclasts, that will make it difficult to evaluate the main fragmentation process.

Ash particles created by magmatic, MFCI or quench granulation type fragmentation can be distinguished by the different shape and morphology characteristics of the ash particles (Wohletz, 1983; Büttner et al., 1999). However, the discrimination between magmatic and phreatomagmatic derived ash particles using only textures such as hydration cracks, mossy irregular, blocky equant or fluidal shape descriptors, will not give clear results (Dellino and La Volpe, 1996) and will be especially difficult in heterogeneous deposits with ash particles formed by different fragmentation processes. As a solution to this problem, particle shape analysis has been successfully used by many authors (Dellino and La Volpe, 1996; Büttner et al., 2002; Dellino and Liotino, 2002; Ersoy et al., 2006; Cioni et al., 2008; Dürig et al., 2012b) to characterise ash deposits and the ash-forming fragmentation process. One of the main methods, that is proven to give clear results and can be used for the comparison of different ash deposits is the image parameter analysis (IPA) proposed by Dellino and La Volpe (1996)

* Corresponding author.

E-mail address: S.Jordan@opgc.univ-bpclermont.fr (S.C. Jordan).

(Dellino and Liotino, 2002; Zimanowski et al., 2003; Cioni et al., 2008; Dürig et al., 2012b). IPA uses different shape parameters derived from 2D projection of the ash particle, such as rectangularity, circularity, compactness and elongation, to characterise ash particles.

In this study, IPA is used for the comparison of natural ash particles from the pyroclastic Lake Purrumbete maar succession with ash particles derived from standardised fragmentation experiments, simulating both magmatic and phreatomagmatic fragmentation mechanisms. This approach is used to determine the main fragmentation mechanism operating during the Lake Purrumbete eruption, as the shape of the ash particles is considered to be predominantly influenced by the

fragmentation mechanism (Fröhlich et al., 1993; Dellino and La Volpe, 1996; Büttner et al., 2002; Dürig et al., 2012b).

2. Description of the study materials

2.1. Natural ash particles

Seven samples of volcanic ash particles were collected from pyroclastic lapilli-ash and ash deposits of the Lake Purrumbete maar in the Newer Volcanics Province, southeastern Australia (Fig. 1A). Lake Purrumbete is a very large maar complex (>3 km) with multiple

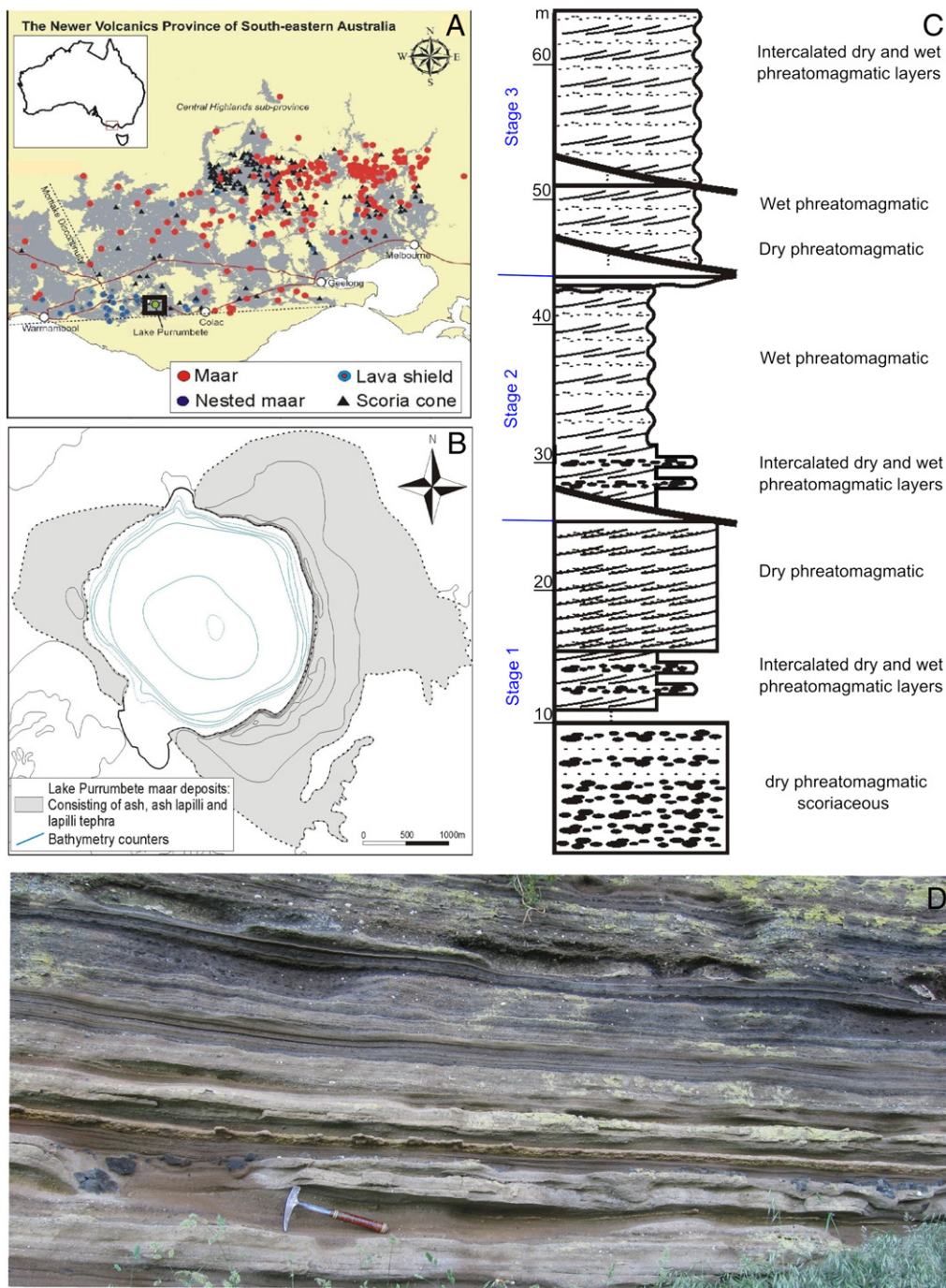


Fig. 1. A) Map of the Newer Volcanics Province, southeastern Australia (modified after (van Otterloo et al., 2013)), B) map of the distribution of the Lake Purrumbete maar deposits (modified after (Jordan et al., 2013)), C) composite stratigraphical log of the Lake Purrumbete maar rim succession (modified after (Jordan et al., 2013)), and D) photograph of the Lake Purrumbete deposits with wet phreatomagmatic fine ash layers at the bottom and coarse grained dry phreatomagmatic scoriaceous deposits at the top.

coalesced craters formed by predominantly phreatomagmatic eruptions and a few phases where the water supply was restricted, resulting in limited phreatomagmatic activity and less efficient fragmentation (Fig. 1B). The eruption took place in three stages, with a significant volcanic hiatus between the second and third stages (Jordan et al., 2013, Fig. 1C). The at least 40 m thick volcanic succession of Lake Purrumbete maar shows the whole range of pyroclastic deposit from wet surge fine ash deposits to dry surge scoriaceous ash–lapilli deposits (Fig. 1D), which has been described in detail by Jordan et al. (2013). The differences in the grain-size of these deposits are the result of changes in the water supply, which was restricted in some of the coalesced craters. The Lake Purrumbete maar is around 50 thousand years old and the brown to yellow colour of the basaltic juvenile particles observed in thin sections indicates some degree of alteration and palagonitisation of the glass. However, the ash particles still show very distinct shapes and morphologies, as can be seen in Fig. 2A of a bulk SEM image of natural Lake Purrumbete ash. For IPA analysis samples were chosen from both end members, the wet surge fine ash deposits (samples: Ash1, Ash2, Ash3, Ash4) and the dry surge scoriaceous lapilli deposit (sample: Scor1) and from the medium range of dry surge ash–lapilli deposits (samples: Lapi1, Lapi2). All natural samples, except for Scor1, were deposited by diluted pyroclastic density currents (PDCs), with fine ash particles being deposited from suspension (Jordan et al., 2013). In addition, the scoriaceous lapilli deposit Scor1 of the Lake Purrumbete succession is classified by Jordan et al. (2013) as a surge modified fallout deposit. The amount of fine ash (<125 µm) varies from almost 90% for the wet surge fine ash deposits to 1–5% for the dry surge ash–lapilli deposits.

Wet surge fine ash deposits contain 60% of equant particles with irregular shapes and a rough surface and 25% of particles that have a blocky shape with a rough surface. Less common (10–15%) are angular and curvi-planar fragments, with a smooth surface. Smooth spherical particles similar to Pele's tears are very rare (less than 1%). Typical textures of magma/water interaction such as quenching cracks and stepped surfaces are minor. Many clasts have a distinct foam like surface texture, which is more predominant in samples of wet surge deposits than in dry surge deposits (Fig. 3). This foam like texture is similar to the chemical pitting textures described by Dellino et al. (2001) and therefore may have been caused by the contact of fluids and hot glass particles. The majority of clasts have smaller particles adhering to the surface, which is characteristic for phreatomagmatic derived clasts (Dellino et al., 2001).

Dry surge ash–lapilli deposits contain the same clast types as wet surge fine ash deposits, but in different abundances. Equant particles with an irregular shape and blocky particles are still abundant with 50–60% and 15–20% abundances. Angular and curvi-planar fragments, however, are more abundant with 20–30% in the wet surge deposits with many particles showing imprints of vesicle textures on the surface. The deposits contain also small amounts of Pele's tears (4–10%) and some elongated particles in the shape of Pele's hairs (Fig. 3).

However, quenching cracks on the particle surfaces indicate some magma/water interaction.

2.2. Experimental ash particles

Fresh, clean and glassy scoria clasts from the Mount Rouse volcanic complex, southeastern Australia were used to create the experimental particles. This material has a similar geochemical composition as the Lake Purrumbete material (Table 1), but is better suited for the experiments than the Lake Purrumbete material itself, because the Mount Rouse material has a larger grain size and is not contaminated with fragmented country rock material, nor does it show signs of hydration and alteration. Prior to the experiments the material was melted in a crucible by induction heating. Three different types of standardised fragmentation experiments were conducted: thermal granulation experiments, dry 'blowout' experiments and wet 'blowout' experiments following the setup of Büttner et al. (2006) and Austin-Erickson et al. (2008) (Fig. 4). In thermal granulation experiments, the melt is poured into water and fragmented by thermal quenching. This experiment can be used as an analogue for the natural process of magma entering a water body and being fragmented by quench fragmentation (Büttner et al., 1999; Austin-Erickson et al., 2008; Schipper et al., 2011; Dürig et al., 2012b).

In dry 'blowout' experiments pressurized gas is injected underneath the melt plug causing it to deform and fragment. Brittle fragmentation of the melt is caused by the high strain rate during deformation within the crucible, with further fragmentation by acceleration of the whole system during ejection out of the crucible, which is driven by the gas pressure (Büttner et al., 2002, 2006). These experiments are used to simulate fragmentation under quasi-isothermal magmatic conditions (Dürig et al., 2012b).

During wet 'blowout' experiments pressurized gas is also injected underneath the melt plug to deform the plug and cause the formation of micro-cracks. Molten fuel coolant interaction (MFCI) was initiated by injecting water into the crucible on top of the melt plug. The large surface, increased by the generated micro-cracks, enhanced the magma water interface leading to explosive fragmentation of the melt plug (Austin-Erickson et al., 2008).

Particles formed during the thermal granulation experiment (sample GT) are exclusively angular with sharp edges and a very smooth, glassy surface (Fig. 5). Concentric fracture marks are a common feature indicating brittle fragmentation.

The majority of particles in the three samples of dry 'blowout' experiments (BL05, BL06 and BL07) are angular with smooth surfaces, vesicle imprints and curvi-planar shapes (42%) or blocky in shape (34%). The samples also contain abundant particles (16%) with a fluidal shape, including stretched, flexed and contorted structures, and elongated or spherical shapes (Figs. 2B and 3), indicating ductile fragmentation (Büttner et al. 2002). Less abundant are sub-rounded to sub-angular

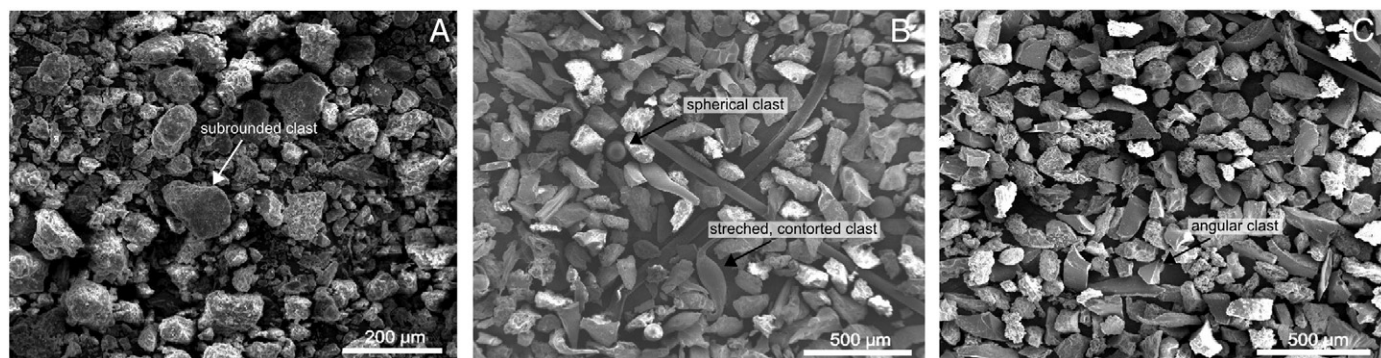


Fig. 2. Bulk SEM images of A) natural Lake Purrumbete ash particles, B) dry 'blowout' ash particles and C) wet 'blowout' ash particles.

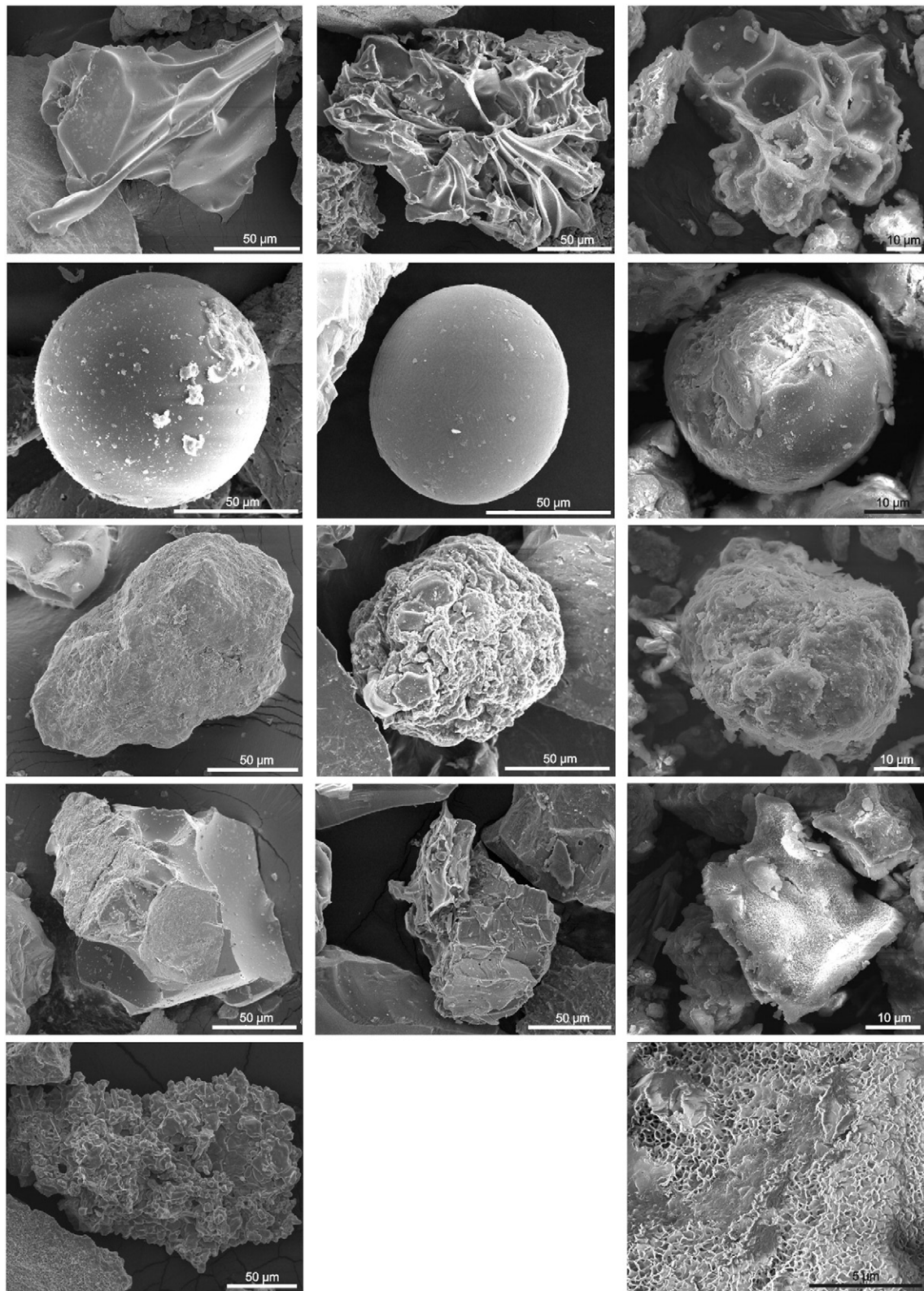


Fig. 3. SEM images of natural and experimental ash particles. First column: particles derived from dry 'blowout' experiments; second column: particles from wet 'blowout' experiments; last column: natural ash particles, with high resolution image of chemical pitting (last image). First row: vesiculated clasts; second row: spherical clasts similar to Pele's tears; third row subrounded clasts with a rough surface; fourth row: angular clasts.

particles with a rough surface (8%, Fig. 3). Cuboid surface structures are also common, while stepped surface structures occur only in minor amounts.

The two samples of wet 'blowout' experiments (MFC1 and MFC2) contain the same range of particle shapes and surface textures as the dry 'blowout' samples, with 46% of angular, 44% of blocky and 3% of

Table 1
General geochemistry of Lake Purrumbete and the Mount Rouse material.

	SiO ₂	TiO ₂	Al ₂ O ₃	Fe ₂ O ₃	MnO	MgO	CaO	Na ₂ O	K ₂ O	P ₂ O ₅	LOI
<i>Mt Rouse</i>											
2208-590	47.62	2.4	13.99	12.2	0.16	8.68	8.19	3.59	1.65	0.66	0.4
<i>Lake Purrumbete</i>											
514	46.5	2.74	14	12.3	0.16	5.68	7.95	4.26	2.72	1.14	2.3
WQ5a	46.1	2.89	13.8	13	0.16	6.99	6.71	3.08	2.4	1.04	3.52

sub-angular particles. However, particles with a fluidal shape are 7% less abundant than in the dry 'blowout' experimental samples (Fig. 2C). On the surface of some particles quenching cracks can be observed.

3. Image particle analysis (IPA)

3.1. Methods

Image particle analysis (IPA) was developed by Dellino and La Volpe (1996) and used by Zimanowski et al. (2003), Cioni et al. (2008) and Dürig et al. (2012b) for comparison of natural and experimentally derived ash particles. Here, the method is used for the analysis of particles sized 130 µm and smaller, as only particles in this size range are actively produced by explosive magma/water interaction (Büttner et al., 2002). The shape parameters of each particle were measured, using binary scanning electron microscope (SEM) images. SEM images of 30 individual particles were acquired per sample, using the JEOL 7001 electron microscope of the Monash Centre of Electron Microscopy with a working distance of 10 mm and an acceleration voltage of 15 kV. The following statistical analysis of the particles uses four adimensional IPA parameters: compactness, rectangularity, elongation and circularity.

Compactness is the ratio of the cross-section area A and the product of breadth b and width w of the smallest bounding box circumscribing the particle (Fig. 6):

$$\text{compactness} = \frac{A}{b * w}. \quad (1)$$

Values for compactness range between 0 and 1, with values close to 1 indicating a particle shape similar to a rectangle.

The rectangularity of a particle shape is defined by the ratio of the particle perimeter p and the perimeter of the bounding box written as:

$$\text{rectangularity} = \frac{p}{2 * b + 2 * w} \quad (2)$$

where b is the breadth and w is the width of the bounding box. Values close to 1 again indicate a particle shape close to a rectangle.

Elongation is specified by:

$$\text{elongation} = \frac{a}{m} \quad (3)$$

with a being the maximum Feret diameter of the particle and m being the mean length of the line segments perpendicular to the maximum intercept, which is equal to particle area/maximum intercept. Circularity is defined by:

$$\text{circularity} = \frac{p}{c} \quad (4)$$

with c being the perimeter of a circle with the same area as the particle itself. As a result, particles with a circularity of 1 are round while more irregular particles will have higher circularity values.

The shape parameters of the samples were compared by using different statistical methods applicable for IPA analysis (Dellino et al., 2001; Büttner et al., 2002; Mele et al., 2011; Dürig et al., 2012b). The samples were first compared by means of using a t -test (test of equality of means). The results of this test show if sample pairs show significant differences. In addition, equivalence tests were run on sample pairs without significant differences in the t -test, to determine significant similarities, meaning that the differences in means lie within the given threshold values of 0.1 for rectangularity and compactness and 0.9 for elongation and circularity (Dürig et al., 2012b).

4. IPA results

The distributions of the IPA parameters of each natural sample were compared to each other using statistical tests such as t -test and equivalence tests. The results of the t -test show that there are no significant differences in the composition of clast shapes between different natural ash samples. Significant similarities in all four IPA

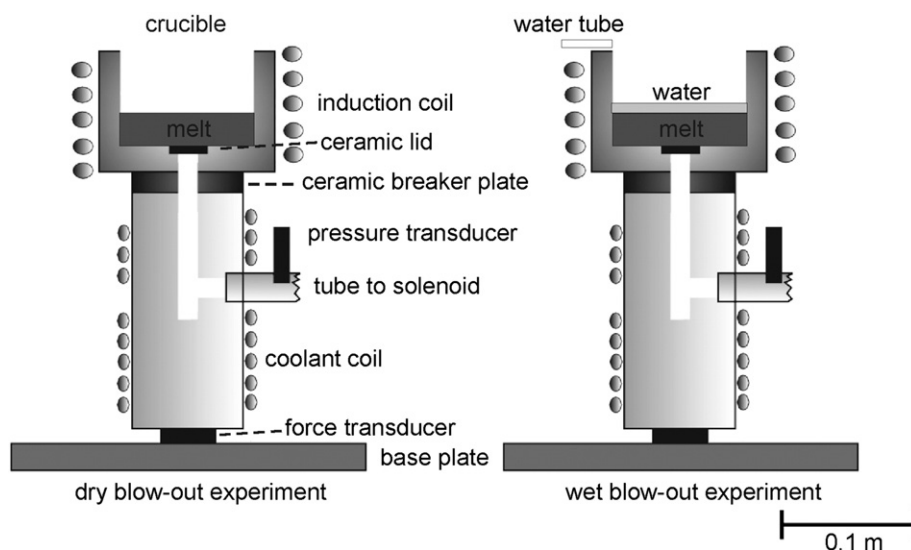


Fig. 4. Experimental set-up of dry and wet 'blowout' experiments. Modified after Büttner et al. (2006) and Austin-Erickson et al. (2008).

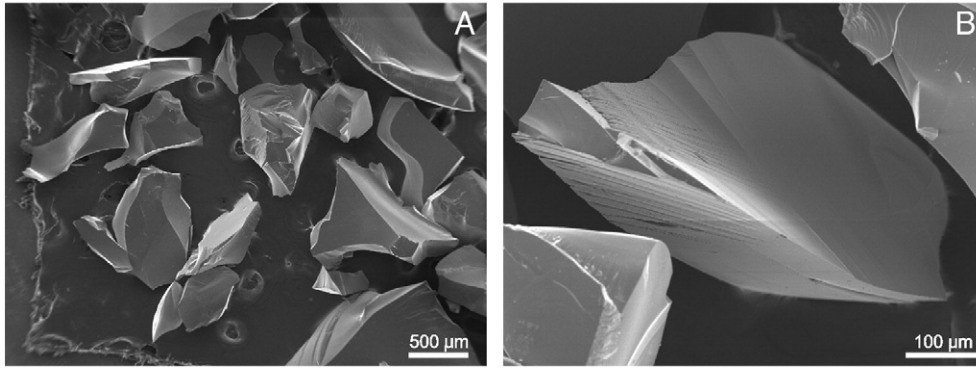


Fig. 5. SEM images of ash particles derived from thermal granulation experiments, with typical angular shape and fracture marks on the smooth surface.

parameters, however, were only verified by the equivalence test for the following samples:

- (1) Lapi1–Ash4
- (2) Lapi2–Ash3.

In addition, for the following data sets a significant similarity is verified for three IPA parameters and cannot be excluded for the fourth one by equivalence tests, which favours the conclusion that an equivalence of shape is highly probable:

- (1) Lapi1–Lapi2
- (2) Lapi1–Ash1
- (3) Lapi1–Ash3
- (4) Ash4–Lapi2.

Comparison of the natural samples to the experimental samples gives different results for the three different types of experiments. The results of the *t*-test show very clearly that particles of the GT sample that were created by thermal granulation have a very different shape compared to the natural ash samples. In addition, the natural clasts show overall distinct differences from the dry ‘blowout’ samples BL05 and BL07, whereas no significant differences were determined by the *t*-test for BL06. The results of the equivalence test, however, confirm significant similarities in all four IPA parameters only for BL07 for the following combinations:

- (1) BL07–Lapi1
- (2) BL07–Ash3
- (3) BL07–Ash4.

Significant similarities in three IPA parameters where the fourth one cannot be excluded by the equivalence test are found for the following two combinations:

- (1) BL06–Ash2
- (2) MFC12–Ash3.

In addition, natural ash samples show only significant differences in one or less IPA parameters compared to the wet ‘blowout’ samples with three natural ash samples (Ash1, Ash2 and Scor1) varying only in the rectangularity parameter from the wet ‘blowout’ samples. This parameter, however, is very susceptible to rounding (Table 2).

An interesting point is that the experimental samples of wet and dry ‘blowout’ experiments show no significant differences with each other except for sample BL07 which is again very different from the rest of the experimental samples, but consistent in the same IPA parameters such as compactness, elongation and circularity. There are no significant differences in the rectangularity between BL07 and the other experimental samples. The differences of BL07 from the other ‘blowout’ experiments are also obvious in the comparison of the dry and wet ‘blowout’ ash particles to the thermal granulation ash particles of sample GT. The GT ash particles differ from the other experimental ash samples only in the rectangularity parameter, whereas BL07 differs in three IPA parameters from GT.

5. Discussion

The overall similar shape of the natural ash samples indicates that they were shaped by the same processes of either fragmentation or transportation. Field evidence, including cross-stratification, dune forms and undulating layers described by Jordan et al. (2013), indicate

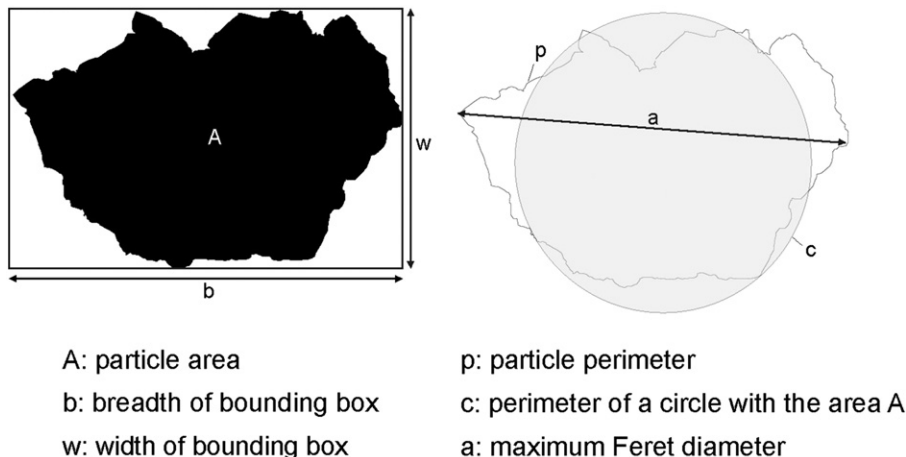


Fig. 6. Definition of the different shape parameters used to calculate IPA parameters.

Table 2

Results of the *t*-test for each sample pair. The table gives the IPA-parameters in which each sample pair differs significantly from each other, where R, Co, Ci and E are rectangularity, compactness, circularity and elongation respectively.

	Scor1	Lapi1	Lapi2	Ash1	Ash2	Ash3	Ash4	MFCI1	MFCI2	BL07	BL06	BL05
GT	R	R,Co,E	R,Co	R	R,Co,E	R,Co	R,Co,E	R	R	R,Co,E	R	R
BL05	R	R,E	0	R,E	R,E	0	Co,E	0	0	Co,E,Ci	0	
BL06	0	E	Co	0	0	0	Co,E	0	0	Co,E,Ci		
BL07	R,Co,Ci	Co*	E	R,Co,Ci	R,Ci	0	0	Co,E,Ci	Co,E,Ci			
MFCI1	R	E	0	R	R	0	E	0				
MFCI2	R	E	Co	R	R	0	Co,E					
Ash4	0	0	0	Co	0	0						
Ash3	R	0	0	R	0							
Ash2	0	0	0	0								
Ash1	0	0	Co									
Lapi2	0	0										
Lapi1	0											

* The value is exactly the threshold value.

that all samples were either deposited by diluted PDCs or were modified by some surge activity, and therefore the particles may be expected to show some signs of physical abrasion. However, the studied particles are in the size range of the fine ash fraction that typically travel in the diluted ash cloud where collision of the particles is rather rare, resulting in only small scale abrasion of the particles. Very small degrees of rounding and abrasion are indicated by the differences in the rectangularity parameter that is the most sensitive IPA parameter to rounding of the particle corners. The overall observed angularity of the particles and their similarity to MFCI ash particles indicate that modification by transport was very minor, as the experimental fragments did not experience any rounding process. This is in agreement with the study of Mattsson (2010) on ash particles from the Capelas tuff cone (Azores) that shows that both fall and surge deposits have the same fractal dimension indicating only minor modification of the ash particles transported by the surges. Mattsson (2010) explains this with the very low concentration of particles in the surge that prevents particle collisions and suggests that this may be different for surges generated by more energetic eruptions such as maar eruptions. The new data presented here shows now that also in surges formed by high energetic maar eruptions the degree of abrasion on the particles is still extremely small.

The Lake Purumbete pyroclastic succession comprises a large variety of deposit types that are considered to be the result of changes in the eruption conditions and the explosion efficiencies due to changes in the availability of water to the phreatomagmatic system (Jordan et al., 2013). It is therefore surprising that overall all natural ash samples are similar indicating that the shaping of the particles is independent of the explosion efficiency, but rather the result of the fragmentation mechanism. Therefore, even if this fragmentation process was less efficient, indicated by a larger mean grain size of the deposits, the fine ash fraction was still formed by the same mechanism as the fine ash generated during very efficient explosions.

Studies by Mattsson (2010) and Graettinger et al. (2013) have shown that particles formed by both magmatic and phreatomagmatic fragmentation types can be present in the same deposit, as the result of a complex interplay of both magmatic and phreatomagmatic explosions. In addition, recycling of pyroclastic material is a major process during maar eruptions and will cause the deposition of clasts that may have not been formed at the same time (Ross and White, 2012 and references therein). The comparison of the natural ash samples with the ash samples of both wet and dry 'blowout' experiments gives information on the main particle forming process. The results of the IPA analysis presented here show that many natural ash samples differ significantly in two or three IPA parameters from samples of dry 'blowout' experiments, suggesting that the Lake Purumbete ash samples were not formed by magmatic fragmentation. This is supported by the relatively small differences (one or less IPA parameter) of all natural ash samples from the MFCI ash particles indicating an origin of

the grain shape by MFCI type fragmentation. This clear difference in the similarity of the Lake Purumbete ash particles to the ash particle populations of the two different experimental set-ups shows that the grain shape of the natural particles is predominantly controlled by the fragmentation mechanism.

The significant differences of the natural samples from the thermal granulation sample clearly show that the natural particles were not formed by thermal granulation and that this process did not occur during the eruption of the Lake Purumbete maar.

All experimental samples show no significant differences with each other except for sample BL07, that differs significantly from the other experimental samples in three parameters, the circularity, compactness and elongation. It should be noted, that there are no differences in the rectangularity between BL07 and any other experimental sample. Sample BL07, however, is the only experimental sample that has significant similarities – verified for all four IPA parameters – to three natural samples. These results lead to the question of why sample BL07 is so different from the rest of the experimental samples.

The answer may be found in the pressure and force data measured during each experiment by a pressure transducer attached to the gas injection tube and a force transducer underneath the crucible (Fig. 4). Fragmentation of the melt plug is indicated by the first strong amplitude of the force signal (Dürig et al., 2012a). The pressure and force diagrams of the experiments (Fig. 7) clearly show, that experiment BL07 is the only experiment where fragmentation of the melt occurred after a longer time frame (BL07: 0.05 s) after initiation of deformation and at higher pressures (>100 bar) than the other experiments (0.02–0.03 s, 40–50 bar). As a result, melt plug BL07 was deformed and strained to a greater extent than the melt plugs in the other experiments, indicated by the longer time frame and the higher accommodated pressure. These differences in the degree of deformation and strain may be the reason for the significant differences in the particle shape of BL07 from the other experiments. Dürig et al. (2012b) explained differences in IPA parameters of natural and experimental MFCI particles with pre-stresses that influence largely the formation of the particles and their shapes. During the here presented experiments stress is created before fragmentation by the deformation and straining of the melt plug. Therefore it can be assumed that these pre-stresses in the melt plug were higher during the BL07 experiment with a long time frame for deformation and higher accommodated pressures than in the other experiments, resulting in significantly different IPA parameters of circularity, compactness and elongation. The pre-stress seems to have no influence on the rectangularity of the ash particles, as there were no significant differences detected by the *t*-test in the rectangularity of the ash particles of different experimental samples. These results show that in the experimental set-up the degree of stress prior to fragmentation has more influence on the resulting particle shape than the fragmentation mechanism, as samples of both dry and wet 'blowout'

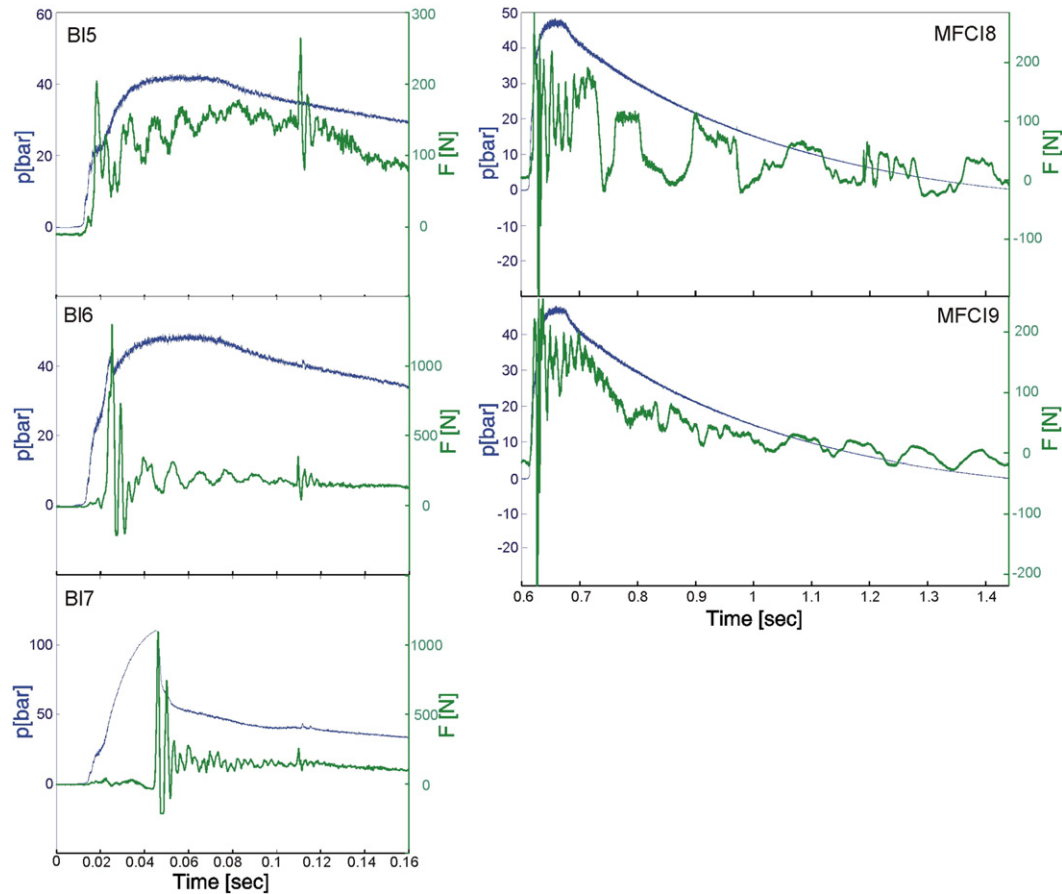


Fig. 7. Diagrams of the plotted data recorded by the force and pressure transducers. Experimental run BL05 shows that acceleration of the melt plug failed at the beginning with further pressure built up and fragmentation, indicated by second peak of the force graph. Both experimental runs BL06 and BL07 show a first fragmentation event indicated by the first peak in the force graph, followed by closure of the system and a later second fragmentation event (second peak in the force graph). Early fragmentation due to magma/water interaction is indicated for both experimental runs MFCI8 and 9 by the strong peaks in the force graph prior to the peak in the pressure graph.

experiments such as MFCI1, MFCI2, BL05 and BL06 are not significantly different.

The results of the *t*-test give 34 sample pairs that show no significant differences and therefore seem to be similar in their overall grain shape. As discussed above these similarities seem to be the result of the formation of the ash particles by the same fragmentation mechanism. However, most of these sample pairs were disregarded by the equivalence test, that left only five sample pairs with significant – in the sense of statistically verifiable – similarities. These variations in the shape that are the reason why the majority of the samples are not significantly similar, must be extremely small, otherwise they would have been indicated by the *t*-test (Table 3). Dellino and Liotino (2002) found in their study of magmatic and phreatomagmatic ash particles from Monte Pilato-Rocche Rosse, Italy, two orders of irregularities on the surface of magmatic ash particles defined by two different fractals, one large scale fractal caused by the vesicle imprints and one small scale fractal caused by very small irregularities. They showed that this small scale fractal is similar to the fractal of phreatomagmatic particles and suggested that this is caused by the same rheological behaviour of the melt. The work presented here also indicates two orders of irregularities, more prominent irregularities that can be detected by the *t*-test and very small irregularities that can only be detected using equivalence tests. As these very small irregularities vary between different experimental samples they cannot be only the result of the rheological behaviour of the melt, as the same material was used for all experiments. The work presented here suggests that differences in the pre-fragmentation conditions, especially in the strain rate, may cause the formation of these small irregularities. These variations in the pre-fragmentation

conditions can be assumed to be present, as each explosion in both natural conduits and experimental crucibles is unique. As a result it can be said, that the fragmentation process seems to control the overall grain shape, whereas existing pre-stresses cause small variations in the grain shape. It is striking, that in five of the six cases, a significant similarity is rejected by the equivalence test results because of variations in the elongation parameter. This could be an indication that the elongation is the parameter that is the most affected by slight variations in pre-fragmentation conditions such as the degree of pre-stress.

6. Conclusions

The results show that the particle shape is created mainly by the fragmentation process and therefore predominantly influenced by the type of fragmentation, which is in agreement with the results of the study of Dürig et al. (2012b), which showed that the particle shape is strongly dependent on the fracture mechanism.

The comparison of experimental and natural ash particles with IPA parameters can be used to identify the predominant fragmentation mechanism that has formed the particles. In the case of the Lake Purrumbete maar samples, the majority of the fine ash fraction of all sampled deposits has been formed by phreatomagmatic MFCI type fragmentation, with only a minor fraction being formed by magmatic brittle type fragmentation. This is in agreement with the field observations of diluted PDCs described by Jordan et al. (2013) and typical for phreatomagmatic maar eruptions.

The experimental results indicate that pre-stresses within the melt prior to fragmentation also have an influence on the particle shape,

Table 3

Results of the equivalence tests. Comparison of the sample pairs is done for each IPA parameter, using threshold limits defined by Dürig et al. (2012b). Significant similarity of samples is indicated with 'yes', no similarity is shown by 'no' and () means no statement can be made about the similarity of the samples, as the variances within each sample are not comparable.

Set 1	Set 2	Rect = 0.1	Comp = 0.1	Elong = 0.9	Circ = 0.9
BL05	Lapi2	Yes	()	()	()
BL05	Ash3	Yes	()	()	()
BL05	BL06	()	Yes	No	Yes
BL05	MFC11	Yes	Yes	No	()
BL05	MFC12	Yes	()	()	()
BL06	Scor1	()	Yes	No	Yes
BL06	Ash1	()	Yes	()	()
BL06	Ash2	Yes	Yes	()	Yes
BL06	Ash3	()	Yes	()	()
BL06	MFC11	()	Yes	No	Yes
BL06	MFC12	()	Yes	No	Yes
BL07	Ash3	Yes	Yes	Yes	Yes
BL07	Ash4	Yes	Yes	Yes	Yes
BL07	Lapi1	Yes	Yes	Yes	Yes
MFC11	Lapi2	Yes	Yes	()	()
MFC11	Ash3	Yes	()	()	Yes
MFC12	Ash3	Yes	Yes	Yes	()
Scor1	Lapi1	Yes	()	()	()
Scor1	Lapi2	Yes	Yes	()	()
Scor1	Ash1	Yes	Yes	()	()
Scor1	Ash3	()	Yes	()	Yes
Scor1	Ash4	()	()	()	Yes
Lapi1	Lapi2	Yes	Yes	()	Yes
Lapi1	Ash1	Yes	Yes	()	Yes
Lapi1	Ash2	()	()	()	()
Lapi1	Ash3	Yes	Yes	()	Yes
Lapi1	Ash4	Yes	Yes	Yes	Yes
Lapi2	Ash3	Yes	Yes	Yes	Yes
Lapi2	Ash4	Yes	Yes	()	Yes
Ash2	Ash1	()	Yes	Yes	()
Ash2	Ash3	()	Yes	Yes	()
Ash2	Ash4	No	()	()	()
Ash3	Ash4	Yes	()	Yes	()

although to a smaller degree than the fragmentation mechanism. The rectangularity of the particles, however, is formed independently of the pre-stress and is more affected by rounding (such as in secondary abrasion processes).

t-Tests in combination with equivalent tests indicate very fine variations between particle populations. These variations in shape might have been caused by differing conditions prior to fragmentation such as pre-stress. Each fragmentation process either in the experimental crucible or in the natural conduit is unique and therefore it is very likely that the resulting particle shape populations have very slight differences that can be revealed by statistical analysis of their IPA parameters. The elongation of the particle seems to be especially sensitive to slight changes in the fragmentation conditions.

Acknowledgements

The research of S. C. Jordan was supported financially by a scholarship from the Monash University and a scholarship from the Faculty of Science at Monash University and discretionary research funds of Ray Cas. We thank the journal reviewers Roberto Sulpizio and an anonymous reviewer

for the useful and improving comments. We are further very grateful for the careful editorial handling by the journal editor Lionel Wilson.

References

- Austin-Erickson, A., Büttner, R., Ort, M.H., Zimanowski, B., 2008. Phreatomagmatic explosions of rhyolitic magma: experimental and field evidence. *J. Geophys. Res.* 113 B11201.
- Büttner, R., Dellino, P., Zimanowski, B., 1999. Identifying magma–water interaction from the surface features of ash particles. *Nature* 401, 688–690.
- Büttner, R., Dellino, P., La Volpe, L., Lorenz, V., Zimanowski, B., 2002. Thermohydraulic explosions in phreatomagmatic eruptions as evidenced by the comparison between pyroclasts and products from Molten Fuel Coolant Interaction experiments. *J. Geophys. Res.* 107 (B11).
- Büttner, R., Dellino, P., Raue, H., Sonder, I., Zimanowski, B., 2006. Stress-induced brittle fragmentation of magmatic melts: theory and experiments. *J. Geophys. Res.* 111.
- Cioni, R., D'Orlando, C., Bertagnini, A., 2008. Fingerprinting ash deposits of small scale eruption by their physical and textural features. *J. Volcanol. Geotherm. Res.* 177, 277–287.
- Dellino, P., La Volpe, L., 1996. Image processing analysis in reconstructing fragmentation and transportation mechanisms of pyroclastic deposits. The case of Monte Pilato–Rocche Rosse eruptions, Lipari (Aeolian islands, Italy). *J. Volcanol. Geotherm. Res.* 71, 13–29.
- Dellino, P., Liotino, G., 2002. The fractal and multifractal dimension of volcanic ash particles contour: a test study on the utility and volcanological relevance. *J. Volcanol. Geotherm. Res.* 113, 1–18.
- Dellino, P., Isaia, R., La Volpe, L., Orsi, G., 2001. Statistical analysis of textural data from complex pyroclastic sequences: implications for fragmentation processes of the Agnano-Monte Spina Tephra (4.1 ka), Phlegraean Fields, southern Italy. *Bull. Volcanol.* 63, 443–461.
- Dürig, T., Dioguardi, F., Büttner, R., Dellino, P., Mele, D., Zimanowski, B., 2012a. A new method for the determination of the specific kinetic energy (SKE) released to pyroclastic particles at magmatic fragmentation: theory and first experimental results. *Bull. Volcanol.* 74, 895–902.
- Dürig, T., Mele, D., Dellino, P., Zimanowski, B., 2012b. Comparative analyses of glass fragments from brittle fracture experiments and volcanic ash. *Bull. Volcanol.* 74, 691–704.
- Ersoy, O., Chinga, G., Aydar, E., Gourgaud, A., Cubukcu, H.E., Ulusoy, I., 2006. Texture discrimination of volcanic ashes from different fragmentation mechanisms: a case study, Mount Nemrut stratovolcano, eastern Turkey. *Comput. Geosci.* 32, 936–946.
- Fröhlich, G., Zimanowski, B., Lorenz, V., 1993. Explosive thermal interactions between molten lava and water. *Exp. Thermal Fluid Sci.* 7, 319–332.
- Graettinger, A.H., Skilling, I., McGarvie, D., Höskuldsson, 2013. Subaqueous basaltic magmatic explosions trigger phreatomagmatism: a case study from Askja, Iceland. *J. Volcanol. Geotherm. Res.* 264, 17–35.
- Jordan, S.C., Cas, R.A.F., Hayman, P.C., 2013. The origin of a large (>3 km) maar volcano by coalescence of multiple shallow craters: Lake Purrumbete maar, southeastern Australia. *J. Volcanol. Geotherm. Res.* 254, 5–22.
- Mattsson, H.B., 2010. Textural variation in juvenile pyroclasts from an emergent, surtseyan-type, volcanic eruption: the Capelas tuff cone, Sao Miguel (Azores). *J. Volcanol. Geotherm. Res.* 189, 81–91.
- Mele, D., Dellino, P., Sulpizio, R., Braia, G., 2011. A systematic investigation on the aerodynamics of ash particles. *J. Volcanol. Geotherm. Res.* 203, 1–11.
- Ross, P.-S., White, J.D.L., 2012. Quantification of vesicle characteristics in some diatreme-filling deposits, and the explosivity levels of magma–water interactions within diatremes. *J. Volcanol. Geotherm. Res.* 245–246, 55–67.
- Schipper, C.I., White, J.D.L., Zimanowski, B., Büttner, R., Sonder, I., Schmid, A., 2011. Experimental interaction of magma and “dirty” coolants. *Earth Planet. Sci. Lett.* 303, 323–336.
- van Otterloo, J., Cas, R.A., Sheard, M.J., 2013. Eruption processes and deposit characteristics at the monogenetic Mt. Gambier Volcanic Complex, SE Australia: implications for alternating magmatic and phreatomagmatic activity. *Bull. Volcanol.* 75 (8), 1–21.
- Wohletz, K.H., 1983. Mechanics of hydrovolcanic pyroclast formation: grain-size, scanning microscopy, and experimental studies. *J. Volcanol. Geotherm. Res.* 17, 31–63.
- Yew, C.H., Taylor, P.A., 1994. A thermodynamic theory of dynamic fragmentation. *In: J. Impact Eng.* 15 (4), 385–394.
- Zimanowski, B., Büttner, R., Lorenz, V., Häfele, H.-G., 1997. Fragmentation of basaltic melt in the course of explosive volcanism. *J. Geophys. Res.* 102, 803–814.
- Zimanowski, B., Wohletz, K., Dellino, P., Büttner, R., 2003. The volcanic ash problem. *J. Volcanol. Geotherm. Res.* 122, 1–5.